

Conductance Distribution Between Hall Plateaus

Yshai Avishai^{1,2}, Yehuda Band³, and David Brown⁴

¹*Department of Physics, Ben Gurion University of the Negev, Beer-Sheva 84 105, Israel*

²*NTT Basic Research Laboratories, 3-1 Morinosato, Wakamiya, Atsugi-shi Kanagawa-ken, Japan*

³*Department of Chemistry, Ben Gurion University of the Negev, Beer-Sheva 84 105, Israel*

⁴*Goddard Institute for Space Studies, 2880 Broadway, New York, NY 10025*

Mesoscopic fluctuations of two-port conductance and four-port resistance between Hall plateaus are studied within a realistic model for a two-dimensional electron gas in a perpendicular magnetic field and a smooth disordered potential. The two-port conductance distribution $P(g)$ is concave between $g = 0$ and $g = 1$ and is nearly flat between $g = 0.2$ and $g = 0.8$. These characteristics are consistent with recent observations. The distribution is found to be sharply peaked near the end-points $g = 0$ and $g = 1$. The distribution functions for the three independent resistances in a four-port Hall bar geometry are, on the other hand, characterized by a central peak and a relatively large width.

I. INTRODUCTION

The dimensionless conductance g of small metallic disordered systems at very low temperature (where the phase-coherence length is larger than the linear size of the system), is characterized by its distribution $P(g)$ which is nearly Gaussian with mean value proportional to the size of the system and variance of order unity. These properties, also termed as universal conductance fluctuations, are valid deep inside the metallic regime, for which $g \gg 1$. The question whether such (or different) fluctuations occur also in the critical regime where g is of the order of unity has been addressed in connection with the Anderson metal insulator transition prevailing in three-dimensional disordered systems [1]. In this case the critical region can be approached from the metallic side using scaling arguments and expansion in $1/g$. Unfortunately, this is not possible in the quantum Hall regime, since insulating phases exist on both sides of the critical point.

In a recent experiment [2] the conductance distribution function at the quantum Hall transition point was elucidated. The geometry of the experiment was that of a two-dimensional strip with two-ports, namely, one source and one drain. The transition point is defined as that value of the magnetic field for which the averaged conductance is $(n+1/2)\frac{e^2}{h}$. (Since the focus of study is mesoscopic fluctuations, the notion of transition point is more appropriate than that of critical point, which, strictly speaking, applies only in the thermodynamic limit). It was found that in the range of values $0.1 < g < 0.9$ the distribution $P(g)$ is roughly flat. Subsequent theoretical work was mostly based on the network model [3]. The qualitative features of the experimental distribution have been obtained by numerical calculations [4] based on the network model with free boundary conditions on the transverse coordinate. Calculations were performed also with periodic boundary conditions in order to elucidate the role of edge states. Roughly speaking, adopting free (periodic) boundary conditions corresponds to calculating R_{xy} (R_{xx}). Evaluation of $P(g)$ using real space renormalization group methods applied to the network model resulted in a concave shape with a very flat bottom [5,6] and sharp peaks near $g = 0$ and $g = 1$. It is therefore interesting to check (against other models) whether the network model which proves to be extremely successful in describing the critical behavior of the integer quantum Hall effect is also capable of encoding the correct statistical properties of the conductance for mesoscopic systems.

A natural extension of the physics discussed above is related to the mesoscopic fluctuations of the Hall resistance. To the best of our knowledge, investigation of the Hall resistance fluctuations in the transition points between Hall plateaus has not yet been reported. It might be worth pointing out here that the precise relation between the two-port conductance g , discussed in connection with the experiment of Ref. [2], and the conductivity tensor $\sigma_{\mu\nu}$, defined through the Kubo formula, is not unambiguously clear. In particular, an interesting sum-rule relates the two-port transmission coefficient to a *combination* of Hall and dissipative resistivities [7]. This relation holds, in fact, not only at the transition region between plateaus. In order to separate the effects of the Hall and dissipative resistivities a *multi-probe* measurement is required, as employed in the original experiment [8]. Once a multi-probe geometry is defined, numerous resistances can be determined (beside the Hall resistance).

In order to address these questions, calculations of conductance (resistance) distributions between Hall plateaus for two (four) port setups are presented below (in the four-probe geometry, the appropriate quantity is in fact the resistance). The Schrödinger equation for an electron moving in part of the plane restricted by certain boundaries and subject to a strong perpendicular magnetic field and a smooth disordered potential is solved, and transmission and reflection coefficients between various ports are computed [9,10]. The two-

port conductance is calculated using the Landauer [11] formula, while the various four-probe resistances are calculated from the Büttiker formula [12]. Note that no projection on lowest Landau level is made.

We find that the distribution $P(g)$ of the two-port conductance is concave, with rather shallow minimum at $g = 1/2$. As we have already pointed out, the experimental data indicate a flat distribution between $g = 0.1$ and $g = 0.9$, and in this domain the calculated distribution is quite smooth and hence qualitatively accounts for the experimental distribution. On the other hand, there is so far no experimental evidence for the occurrence of two peaks near $g = 0$ and $g = 1$. It is also found that conductances $g(E_F, H)$ at different points of the fermi energy (E) and magnetic field (H) are correlated if the two points are along a transition line.

In the four-probe geometry there are three independent resistances that can be measured, $R_{12,34}$, $R_{13,24}$ and $R_{13,13}$. In this notation $R_{ij,kl}$ is the ratio of the voltage difference between ports i and j and the current flowing between ports k and l . Inspecting the histograms of these three independent resistances at the transition point (defined by $\langle R_{13,24} \rangle = 0.6 \frac{h}{e^2}$), show that all three of them have a distribution which is, more or less, close to a normal one. The width of $R_{12,34}$ (the so called bend resistance) is of order $\Delta R = 0.2h/e^2$ while for $R_{13,24}$ (the Hall resistance), and $R_{13,13}$ the order of the width is $\Delta R = 0.5h/e^2$. This is quite large compared with the corresponding average. Thus, within the realm of mesoscopic fluctuations, the Hall resistance is not a universal number. We are unaware of an experiment aimed at studying mesoscopic fluctuations of multi-probe resistances.

The method of calculation is briefly explained in Sec. II, and the results are presented and discussed in Sec. III.

II. FORMALISM

The two-port system is schematically displayed in Fig. 1a. It consists of a strip $-\infty < x < \infty$, $-L/2 \leq y \leq L/2$ which confines the motion of electrons whose wave function vanishes on the walls. The four-port system is schematically displayed in Fig. 1b. It consists of two perpendicular strips of width L which intersect each other. It is convenient to number the ports (leads) from the left in a counter clockwise sense, so lead number 1 is the left lead *etc.*. In both two and four-port systems, the motion of the electron is ballistic except within the domain $(-L/2 \leq x \leq L/2, -L/2 \leq y \leq L/2)$ where the electron is subject to a smooth disordered potential, defined below. The system is subject to a strong perpendicular magnetic field. It is useful in this geometry to define the vector potential \mathbf{A} in the Landau gauge, $A_x = -Hy$, where H is the magnetic field strength. On this square one considers a

lattice of N^2 Gaussian potentials of width σ , centered at the points $(x_n, y_m) = (-L/2 + a/2 + (n-1)a, -L/2 + a/2 + (m-1)a)$, with $n, m = -N/2 + 1, \dots, N/2$, assuming that $N = L/a$ is an even integer. The random potential is written as

$$V(x, y) = \sum_{nm} v_{nm} \exp\left(-\frac{(x-x_n)^2 + (y-y_m)^2}{2\sigma^2}\right). \quad (1)$$

The impurity strengths v_{nm} are independent random energies, distributed (for convenience) uniformly between $-w/2$ and $w/2$. For this distribution one has

$$\langle v_{nm} \rangle = 0, \quad (2)$$

and

$$\langle v_{nm} v_{n'm'} \rangle = \frac{w^2}{12} \delta_{nn'} \delta_{mm'}. \quad (3)$$

The single-particle reduced Hamiltonian then reads

$$\mathcal{H} = \frac{\hbar^2}{2m} \left[\left(-i \frac{\partial}{\partial x} - \frac{y}{\ell_H^2} \right)^2 - \frac{\partial^2}{\partial y^2} \right] + V(x, y) \equiv \mathcal{H}_0 + V. \quad (4)$$

The magnetic length is given by $\ell_H = (\hbar c/eH)^{1/2}$, where $-e < 0$ is the charge of the electron.

In order to calculate transmission and reflection coefficients one needs to obtain the asymptotic states away from the central region, i.e., in the leads. Consider for example the left lead $-\infty < x < -L/2, -L/2 < y < L/2$. For a given Fermi-energy E_F the solution of the free Schrödinger equation $\mathcal{H}_0 \Psi = E_F \Psi$ in this domain is given by

$$\psi_n^\pm(x, y) = q_n^{-1/2} e^{\pm i q_n (x+L/2)} f(y; \pm q_n), \quad (5)$$

where $f(y; q)$ is a linear combination of parabolic cylinder functions [13] such that the boundary conditions $f(-L/2; q) = f(L/2; q) = 0$ determine the eigen-momenta $q_n(E_F, H)$. Note that in the case of a four-port system, the role of x and y is interchanged in the vertical leads. For convenience, the amplitude of the incident plane wave is set to be exactly unity on the boundaries between the ideal conductors and the region of impurities.

It is worth mentioning that for the present geometry, it is not possible to impose periodic boundary conditions in the transverse direction. This situation is distinct from the one encountered in the network model [3].

The number M of open channels is the maximum number of positive momenta. It is an increasing number of the Fermi-energy E_F and a decreasing number of the magnetic field H . The behavior of the momenta $q_n(E_F, H)$ as function of the two parameters has been discussed elsewhere [9].

Consider now a solution of the full scattering problem such that there is an incoming wave ψ_n^+ of unit amplitude in one of the leads (say lead i), and outgoing waves in all leads j (including the lead $j = i$). The wave function in lead j is then given by,

$$\Psi_n^{ji} = \sum_{m=1}^M \psi_m^+ t_{mn}^{ji}, \text{ (for } j \neq i), \quad (6)$$

and

$$\Psi_n^{ii} = \psi_n^+ + \sum_{m=1}^M \psi_m^- t_{mn}^{ii}. \quad (7)$$

The matrices t_{mn}^{ji} and t_{mn}^{ii} are transmission reflection amplitudes respectively. Within linear response formalism, the two-port conductance g and the four-port resistance tensor $R_{ij,kl}$ can be determined by these amplitudes. In the first case the relation is given by $g = \text{Tr}[t^{12}t^{12\dagger}]$ while in the second case the relation is given in Ref. [12]. The essential part is: $R_{ij,kl} \propto (T^{ki}T^{lj} - T^{kj}T^{li})$, where $T^{ki} = \text{Tr}[t^{ki}t^{ki\dagger}]$.

We recently introduced a variational algorithm for the generalized Z-matrix which, given a finite region in configuration space, effects the following transformation of the scattering wave-function on the boundary surface:

$$\mathbf{Z}(a\Psi(S) + bD\Psi(S)) = d\Psi(S) + qD\Psi(s). \quad (8)$$

In the above we define the generalized normal derivative $D\Psi(S) = \mathbf{n} \cdot \frac{i}{\hbar}\pi\Psi(S)$, where $\pi = \mathbf{p} - \frac{e}{c}\mathbf{A}$ is the generalized momentum for a particle of momentum \mathbf{p} and charge e in a vector potential \mathbf{A} . The parameters a , b , d , and q are arbitrary except that they obey the constraint $aq - bd = -1$. In all studies we use $a = -q = 1$, $b = d = 0$, for which \mathbf{Z} is the negative of the log-derivative matrix. Actually, we use the inverse of this matrix, as discussed in reference [14], which is the negative of the well-known \mathbf{R} matrix. The notation $\Psi(S)$ indicates that the wave-function is evaluated on the boundary surface S and projected onto a suitable basis defined on the surface. In all studies we use sine functions on the boundaries of the regions in Fig. 1. Using the coefficients of $f(y; \pm q_n)$ in the sine basis, [15] we can plug Eqs. (6) and (7) evaluated on the boundaries of the scattering structures into Equation (8) and solve for the coefficients t_{mn}^{ij} using standard singular-value decomposition algorithms [16].

Because of the large bases required, direct computation of the R-matrix was not convenient. Instead, we used a straightforward extension of a recursive cellular R-matrix algorithm outlined by Nesbet [17]. In the 2-port case, we divided the coordinate x into N_x subregions. On each subregion, we computed an R-matrix using a basis consisting of sine functions in y which go to zero at $y = \pm \frac{l}{2}$ and a Legendre discrete variable representation (DVR) in

x [18] (for a discussion of the Legendre DVR we used, see Ref. [14]). Using the continuity and differentiability requirements on Ψ at the boundaries between cells, we concatenated adjacent R-matrices into global R-matrices for the entire region, as discussed by Nesbet.

In the 4-port case, we divided the region in Fig. 1b into N_s^2 square subregions; that is, we divided x and y each into N_s subregions. On each subregion we computed an R-matrix as discussed in Ref. [14] and concatenated them into the global R-matrix for the entire region in a procedure analogous to that outlined above. A few cautions may be in order here. First, for the subregion R-matrices we use Legendre functions as surface functions, not sine functions. This modification is necessary since to use sine functions on the subregions would be to imply that the scattering wave-functions are zero at all the points of intersection between any four cells. Second, the scattering wave-function is zero at the four corners of the square in Fig. 1b. These conditions are enforced by means of linear constraints on the wave-functions in the subcells at these corners. Finally, since the final global R-matrix computed in the manner outlined above would be expressed in terms of Legendre functions confined to $4N_s$ subregions on the surface, the resulting matrix must be projected onto the desired surface sine functions.

III. RESULTS

Let us now make a choice of the potential parameters. We first assign a relation between a and σ such that the exponential factor in the overlap integral between Gaussians of two adjacent impurities, calculated to be $2\pi\sigma^2 \exp\left(-\frac{a^2}{4\sigma^2}\right)$ equals $\exp(-1/2)$. Hence, $\sigma = a/\sqrt{2}$. Next, the length of the system L and the density of impurities $\rho \equiv (Na/L)^2$ are determined by the requirement that in the range of pertinent magnetic fields, the length of the system is much larger than the magnetic length and there is about one impurity per magnetic area ℓ_H^2 . We have found that computation time grows quickly with the total number of impurities, N^2 . The present calculations are carried out with $N = 10$. This yields $L \approx 10\ell_H$.

Hereafter we use atomic units; length is given in units of the Bohr radius $r_0 = 0.5292$ Angstrom, energy is expressed in Hartree (1 Hartree (e^2/r_0) = 27.2 eV), and the atomic unit of magnetic field is equivalent to 1715.1 Tesla. Calculations are performed for system width $L = 2078$ Bohr. The value of disorder strength (w) must be commensurate with those of Fermi-energy and magnetic field so that the conductance is mainly dominated by magnetic field effects and not by disorder. We chose $w = 4.26 \times 10^{-5}$ Hartree and require that the Fermi-energy E_F and the magnetic field H will vary in the region for which the transition between the first plateaus to the insulating phase occur. These are $1.3 \times 10^{-5} < E_F < 1.5 \times 10^{-5}$ and $3.45 \times 10^{-3} < B < 3.80 \times 10^{-3}$ respectively.

A. Two-Port System

First we show in Fig. 2 the two-port average conductance together with its variance near the last plateau. This figure shows that mesoscopic fluctuations occur mainly in the region of transition between plateaus, in agreement with experiment [2]. The distribution $P(g)$ of the two-port conductance is displayed in Fig. 3 for three values of the magnetic field for which the average value of the conductance is 0.514, 0.498 and 0.478. In all three cases the distribution is concave with very shallow minimum at the center and maxima at the endpoints $g = 0$ and $g = 1$. The region between $g = 0.2$ and $g = 0.85$ is roughly flat, in agreement with experiment [2]. Note that the distribution presented here is similar to the one predicted from the network model using the renormalization group technique [5,6]. On the other hand, its characteristics near the end-points is distinct from the one obtained by numerical solution of the network model (see Fig. 5b in Ref. [4]). Assuming the latter procedure to be more accurate than the renormalization group one, we suspect that the network model and the present strip geometry model yield distributions which are very similar in the main part of the interval $0 < g < 1$, but are disparate around the end-points. On the other hand, the results of the present model are in good agreement with RG analysis of the network model. The question which one is closer to the real distribution requires further experimental study.

Another question which is interesting in this context is whether conductances $g(E_F, H)$ at different points in the (E_F, H) plane are correlated. Preliminary results indicate that the answer to this question is affirmative [20]. A useful concept in mesoscopic physics is that of ergodicity, which roughly speaking, implies that fluctuations (of various quantities such as the conductance) as function of a given parameter are equivalent to sample-to-sample fluctuations. The experiment discussed here [2] is based on this hypothesis, since measurements are performed on a single sample at many values of the magnetic field. In other words, it is tacitly assumed that, in the thermodynamic limit, $\langle g(E_F, H)g(E'_F, H') \rangle$ decreases very rapidly with increasing $|E_F - E'_F|$. The question that can be posed here is whether nontrivial correlations $\langle g(E_F, H)g(E'_F, H') \rangle$ do exist. Within the limitation on system size as explained above it is not possible to give a definite answer here. Instead, we display in Fig. 4 a contour plot of $\partial g/\partial H$ in the (E_F, H) plane. The regions of maximal derivatives are clearly shown in the projected contour plot. In the bulk geometry they simply correspond to the Landau levels $E_n = (n + \frac{1}{2})\hbar\omega$. Here they correspond to transition between n and $n + 1$ edge states. It might then be argued that if (E_1, H_1) and (E_2, H_2) are two different points along one of these lines then the correlation $\langle g(E_1, H_1)g(E_2, H_2) \rangle$ is larger than otherwise. Yet, this analysis is only qualitative. In particular, the experimental analysis of conductance derivative reveals correlation lines which cross each other [20]. Interpretation of these latter

observations apparently goes beyond the single particle picture.

B. Four-Port System

We now present results for resistance distributions in the four-port geometry. As mentioned in the introduction, there are three independent resistances to be studied, $R_{13,24}$ (the Hall resistance), $R_{12,34}$ (the bend resistance) and $R_{13,13}$. Note that the latter should not be confused with the dissipative conductance R_{xx} since current and voltage are measured at the same points in the leads. Calculations (and measurement) of R_{xx} require a six port geometry. This is the reason why, in the present scheme, we can calculate the Hall resistance and not Hall conductance. Nevertheless, the resistance $R_{13,13}$ has a non-trivial physical content of its own [10].

The value of the magnetic field H_c at which the quantum Hall transition occurs is usually determined by that value for which R_{xx} has a sharp peak, or, equivalently, the Hall conductance takes on the values $G_{xy} = n + 1/2$. The corresponding value of the Hall resistance $R_{xy} = \frac{G_{xy}}{G_{xx}^2 + G_{xy}^2}$ at the transition point depends on the corresponding value of G_{xx} . Assuming $G_{xx}(H_c) = 0.5$ [19], implies that at the transition point between $n = 2$ (where $R_{xy} = \frac{\hbar}{2e^2}$) and $n = 1$ (where $R_{xy} = \frac{\hbar}{e^2}$) one has $R_{xy}(H_c) = 0.6\frac{\hbar}{e^2}$ (and not $0.75\frac{\hbar}{e^2}$ as one might be tempted to think). We choose to present our results at this point and not the last transition point since there $R_{xy} = \frac{\hbar}{2e^2}$ exactly as in the plateau.

In Fig. 5 we display the distributions of the three resistances at H_c . All the resistances are characterized by a central peak and small tails. In all three cases, the width of the distribution is of the same order as the average itself, which means that mesoscopic fluctuations are rather significant. We are tempted to conjecture that the distribution of the Hall conductance would be similar to that of the Hall resistance, which, comparing with Fig. 3 is much distinct from that found for a two-port system. This is quite significant since, based on the edge state picture, it is intuitively suggestive that two-port magneto-conductance at strong magnetic field is the same as the Hall conductance, which just counts the number of edge states. This is definitely true in the plateau regions, and apparently also in the transition region if the *average* quantity is considered. On the other hand, the pertinent mesoscopic fluctuations are distinct. We have yet to find an explanation for this difference. Unfortunately, measurements of resistance fluctuations in multi-port systems are not yet available.

In conclusion, we have presented a study of conductance and resistance distribution functions in the quantum Hall regime, using a realistic calculation scheme. The two-port conductance distribution agrees well with the experimental one [2]. Its behavior is charac-

terized by a concave shaped curve which is rather flat at the center and sharply peaked near the end-points $g = 0$ and $g = 1$. Our result also indicate possible correlations of conductances at different points in the (E, H) plane, if these points are located on a transition line. The four-port resistance distributions are peaked at their respective central values and have large widths (compared with their mean values). It remains to be determined whether these fluctuations survive in the thermodynamic limit at zero temperature.

ACKNOWLEDGMENTS

This work was supported in part by grants from the Israel Academy of Science *Centers of Excellence*, the DIP program for German Israel Scientific Cooperation, and the US-Israel Binational Science Foundation. We are grateful to J. T. Chalker D. Cobden, E. Kogan and D. Shahar for discussions and suggestions.

-
- [1] B. I. Shklovskii, B. Shapiro, B. R. Sears, P. Lambriandes and B. H. Shore, Phys. Rev. **B47**, 11487 (1993).
 - [2] D. H. Cobden and E. Kogan, Phys. Rev. **B54**, 17316 (1996)
 - [3] J. T. Chalker and P. D. Coddington, J. Phys. **C21**, 2665 (1988).
 - [4] S. Cho and M. P. A. Fisher, Phys. Rev. **B55**, 1637 (1997).
 - [5] A. G. Galstyan and M. E. Raikh , Phys. Rev. **56**, 1422 (1997).
 - [6] D. P. Arovas, M. Jahnssen and B. Shapiro, Phys. Rev. **B56**, 4741 (1997).
 - [7] P. Streda, J. Kucera and A. H. MacDonald, Phys. Rev. Lett. **59**, 1973, (1987).
 - [8] K. von Klitzing, G. Dorda and M. Pepper, Phys. Rev. Lett., **44**, 494 (1980).
 - [9] R.L. Schult, H. W. Wyld, and D. G. Ravenhall, Phys. Rev. **B41**, 12760 (1990).
 - [10] Y. Avishai and Y. B. Band, Phys. Rev. Lett. **62**, 2527 (1989).
 - [11] R. Landauer, IBM J. Res. Develop. **1**, 233 (1957); Z. Phys. **B68**, 217 (1987).

- [12] M. Büttiker, Phys. Rev. Lett. **57**, 1761 (1986); M. Büttiker, IBM J. Res. Develop. **32**, 317 (1988).
- [13] M. Abramowich and I. Stegun, *Handbook of Mathematical Functions*, (Dover, NY, 1972), Chapter 19.
- [14] D. Brown, Y. B. Band, and Y. Avishai, Phys. Rev. **B53**, 4855 (1996).
- [15] H. Tamura and T. Ando, Phys. Rev. B **B44**, 1792 (1991), and references therein.
- [16] W. H. Press, S. A. Teukolsky, W. T. Vetterling, and B. P. Flannery, *Numerical Recipes* (Cambridge, Cambridge, 1992), Chapter 2.
- [17] R. K. Nesbet, Phys. Rev. **A38**, 4955 (1988).
- [18] J. C. Light, I. P. Hamilton, and J. V. Lill, J. Chem. Phys. **82**, 1400 (1985).
- [19] Y. Huo, R. E. Hetzel and R. N. Bhatt, Phys. Rev. Lett. **70**, 481 (1993).
- [20] D. H. Cobden, C. H. W. Barnes, C. J. B. Ford, J. T. Nichols and M. Pepper, in ICPS24-Th1-B1 (Jerusalem, Israel 1998); D. H. Cobden, C. H. W. Barnes, C. J. B. Ford, J. T. Nichols and M. Pepper, preprint submitted to World Scientific

IV. FIGURE CAPTIONS

FIG. 1. Sample geometry used in the present calculations. a) Two port system and b) four-port system. The shaded area contains a disorder potential.

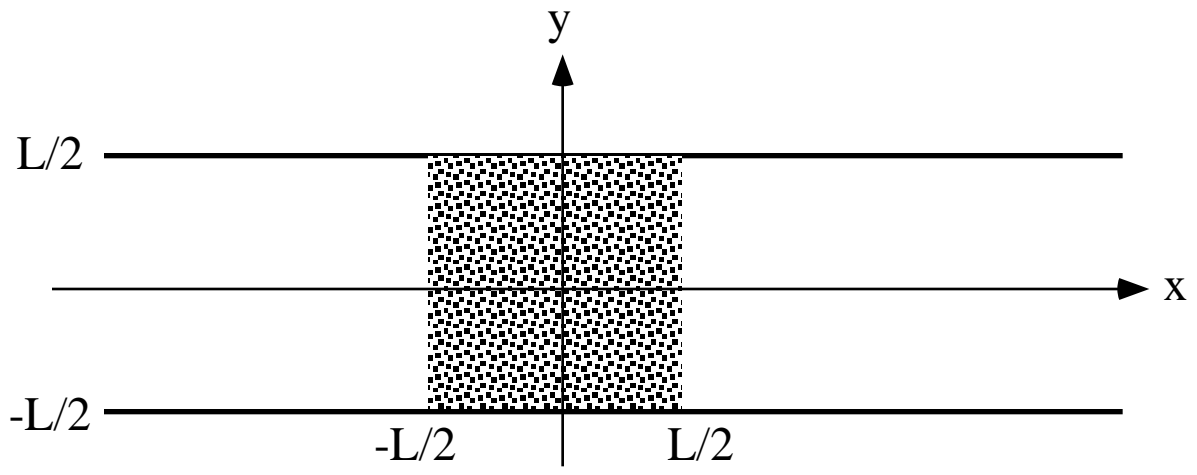
FIG. 2. two-port average conductance (solid line) and its variance (dash-dotted line) as a function of the magnetic field for fixed Fermi energy $E = 3.65 \times 10^{-3}$ Hartree. The system width is $L = 2078$ Bohr, and the disorder strength is $w = 2.3 \times 10^{-5}$ Hartree.

FIG. 3. Distribution $P(g)$ of two-port conductance in the middle of the transition between Hall plateaus $n = 1$ and $n = 0$ for three different values of the magnetic field, $B_1 = 0.00360$ a.u., $B_2 = 0.00365$ a.u. and $B_3 = 0.00370$ a.u. The corresponding values of the average conductances are $g_1 = 0.514$, $g_2 = 0.498$ and $g_3 = 0.478$. Parameters are as in figure 2.

FIG. 4. Three dimensional and contour plot of the conductance derivative $\partial g(E_F, H)/\partial H$ in the (E_F, H) plane for a given sample. Length and disorder parameters are as in Fig. 2. Units of energy and magnetic fields are specified in the text, while g is in units of e^2/h .

FIG. 5. Displayed from top to bottom are distributions of Hall resistance $R_{13,24}$, bend resistance $R_{12,34}$ and the “through” resistance $R_{13,13}$ for $H = 0.00135$ a.u. for which the average value of the Hall resistance is 0.6.

a)



b)

